https://doi.org/10.5194/essd-2023-436
Preprint. Discussion started: 18 December 2023

High resolution observations of the ocean upper layer south of Cape São Vicente, western northern margin of the Gulf of Cadiz.

Sarah A. Rautenbach[1], Carlos Sousa[1,2], Mafalda Carapuço[2], Paulo Relvas[1]

1 Centre of Marine Sciences (CCMAR), Universidade do Algarve, Campus de Gambelas, 8005-139 Faro, Portugal,

2 Portuguese Institute for the Sea and Atmosphere (IPMA, I.P.), Rua C do Aeroporto 1749-077 Lisboa Portugal

Corresponding Author: Sarah Rautenbach, srautenbach@ualg.pt

https://doi.org/10.5194/essd-2023-436
Preprint. Discussion started: 18 December 2023

Open Access Earth System Science Data Discussions

Abstract

This article presents an Eulerian physical and biogeochemical data set from the Iberian Margin Cape São Vicente Ocean Observatory (IbMa-CSV), a facility of the European Multidisciplinary Seafloor and water column Observatory - European Research Infrastructure Consortium (EMSO-ERIC) located 10 nautical miles south of Cape São Vicente (Portugal), the southwest tip of the Iberian Peninsula and western limit of the northern margin of the Gulf of Cadiz. The observatory was installed on the shelf break, and the data time series spans four months for most of the variables. The upper 150 m were sampled intensively with a wave powered vertical profiler at an average rate of 4.5 profiles per hour recording at 2 Hz when ascending at approximate velocity of 0.2 m/s and 10 Hz when descending at variable velocity. The vertical resolution was always higher than 0.2 m. Measured channels were conductivity, temperature, pressure, chlorophyll *a*, dissolved O_2 concentration, and turbidity. Derived channels are sea pressure, depth, salinity, speed of sound, specific conductivity, dissolved O_2 saturation, density anomaly, spiciness and Brunt-Väisälä frequency. The acquired data set includes the flow velocity and direction along the water column, taken from an upward looking 300 kHz Acoustic Doppler Current Profiler (ADCP) recorded every hour for 3 m depth bins extending the same depth range of the vertical profiler. A standard quality control scheme was applied to the data set. The data set is preserved for multiple use and is accessible in the SEANOE repository, under the address: https://www.seanoe.org/data/00836/94769/ (Rautenbach et al., 2022).

Key words: High resolution dataset, vertical profiles, EMSO-ERIC IbMa-CSV observatory, Cape São Vicente, Western Gulf of Cadiz

https://doi.org/10.5194/essd-2023-436
Preprint. Discussion started: 18 December 2023

Open Access Earth System Science Data Discussions

1. Introduction: the relevance of the site location.

The Iberian Peninsula (Figure 1) represents the northern branch of the Canary Current Upwelling System (CCUS), one of the four Eastern Boundary Upwelling Systems (EBUS), along with the Benguela, California and Humboldt or Peru upwelling systems. These systems are characterized by the coastal upwelling of cold nutrient rich subsurface water, driven by the joint action of northerly winds that blow at least during a substantial part of the year, and the Earth's rotation (Ekman mechanism). Therefore, those systems are among the most productive of the world ocean, which justifies their socio-economic relevance.

The CCUS is unique among the EBUS, since it is the only one punctuated by a discontinuity that is imposed by the entrance of the Mediterranean Sea into the Gulf of Cadiz through the Strait of Gibraltar (Figure 1). The meridional coast of the western Iberian Peninsula is abruptly interrupted at the Cape São Vicente, the southwestern tip of the Iberian Peninsula. There, the coastline turns almost at a right angle into the zonal orientated northern margin of the Gulf of Cadiz.

The continental shelf off the southern part of the western Iberia and in the Cape São Vicente area is narrow (< 10 km wide south of 38° N), approximately delimited by the 200 m bathymetric contour. Over the continental shelf and slope, roughly from April to October, the oceanographic conditions are largely dominated by the upwelling process and associated cold jet flowing equatorward (Relvas and Barton, 2002). For the remainder of the year, the flow is expected to point northward, although there is a lack of observational evidence. Nevertheless, there is measured evidence that over the inner shelf the upwelling pattern is interrupted by the development of a warm coastal counter-current whenever the upwelling favorable winds relax below a certain threshold (Relvas and Barton 2005; Garel et al, 2016).

The Costal Transition Zone, defined as the region where the coastal waters interact with the offshore oceanic waters, is populated by a variety of mesoscale structures, such as meanders, eddies, and filaments. The Cape São Vicente is the root of a recurrent upwelling filament that may extend more than 150 km offshore (Sanchez et al., 2008), exporting to the open ocean a much larger mass than expected by the purely wind-driven Ekman circulation. The new production of an upwelling season could be entirely exported to the open ocean by upwelling filaments (Arístegui et al., 2006), revealing the importance of such features to the ecosystem functioning.

At deeper levels, where the wind is not a forcing factor, the Cape São Vicente region reveals fascinating processes related to the Mediterranean Outflow Water (MOW). After leaping the shallow sill (< 300 m deep) of the Strait of Gibraltar, the salty and warmer MOW sinks sharply into the deep Gulf of Cadiz (depths up to 4000 m), and spreads at depths between 800 and 1200 m, where it finds the equilibrium in the gravitational field (Sanchez et al, 2017). However, a shallow vein detaches and flows at depths as shallow as 400 m or less along the northern continental slope of the Gulf of Cadiz, turning poleward around the Cape São Vicente (Ambar 1983; Cardeira et al., 2013).

https://doi.org/10.5194/essd-2023-436
Preprint. Discussion started: 18 December 2023

Open Access Earth System Science Data Discussions

The higher level of salt entering the North Atlantic through the Strait of Gibraltar and how it spreads throughout the Atlantic basin is a key factor with implications in the functioning of the Atlantic Meridional Overturning Circulation (AMOC), and therefore with climatic consequences. Due to the water column stability, diapycnal mixing of the MOW through entrainment occurs at long time scales when compared with horizontal dispersion through advection (Mauritzen et al, 2001). MOW is dominated by a succession of mesoscale rotating structures, the so called meddies (Mediterranean eddies) (Bower et al., 1995; Ambar et al., 2008). Meddies are described as rotating salt-water lenses, typically 50-200 km wide and 100-200 m thick. There is some evidence that the dynamic effect of meddies propagate along the entire water column, till the surface (Serra et al, 2010). Cape São Vicente is identified as a site for meddy generation. Topographic features along the continental slope near Cape São Vicente are hypothesized as meddy triggers.

Regarding the key role that the Cape São Vicente region plays in a wide variety of oceanographic processes of all scales, some impacting the entire North Atlantic circulation, continuous high resolution and long-term local time series of oceanographic variables are highly valuable for the scientific community and decision makers. Yet, *in situ* observations play a major role in understanding ocean dynamics and can be used for various purposes, until today the availability of continuous and long-term *in situ* data of the ocean is sparse. Off southwestern Iberia, *in situ* observations are limited to event scale records from research cruises. In the frame of the European Multidisciplinary Seafloor and water column Observatory – European Research Infrastructure Consortium (EMSO-ERIC – https://emso.eu/) physical and biogeochemical data from fixed ocean observation platforms throughout Europe are aggregated, harmonized, and shared openly under the CC-BY license, guaranteeing open access for anyone. EMSO-ERIC is a distributed research infrastructure, encompassing observatories and test sites along European waters, from coastal to deep sea locations. Some observatories have already been operating for some time, whereas other nodes are yet to be established. The EMSO-Iberian Margin Cape São Vicente observation platform (IbMa-CSV) is currently producing the first long term set of observations that are presented in this article.

2. Methods

The EMSO-Iberian Margin Cape São Vicente observatory (IbMa-CSV) is located at the southwestern tip of the Iberian Margin, 10 nm south of Cape São Vicente, on the edge of the continental shelf (approximately 200 m depth). A Permit for Private Use of the National Maritime Space (TUPEM) was authorized by the Directorate-General for Natural Resources (DGRM) for an area of 0.35 km^2, in which the observatory is deployed and should not be entered by other parties. However, ship traffic and fishing activities persist to be a risk to the observatory as the TUPEM area is not patrolled. The boundaries of the TUPEM area are 36º50'54.52" N 8º55'37.46" W, 36º50'57.6" N 8º55'13.2" W, 36º50'40.8" N 8º55'40.8" W and 36º50'40.8" N 8º55'13.2" W. Within this area the instruments are fixed on three

https://doi.org/10.5194/essd-2023-436
Preprint. Discussion started: 18 December 2023

separate moorings. The TUPEM is managed by the Center of Marine Science (CCMAR), University of Algarve, Faro, Portugal.

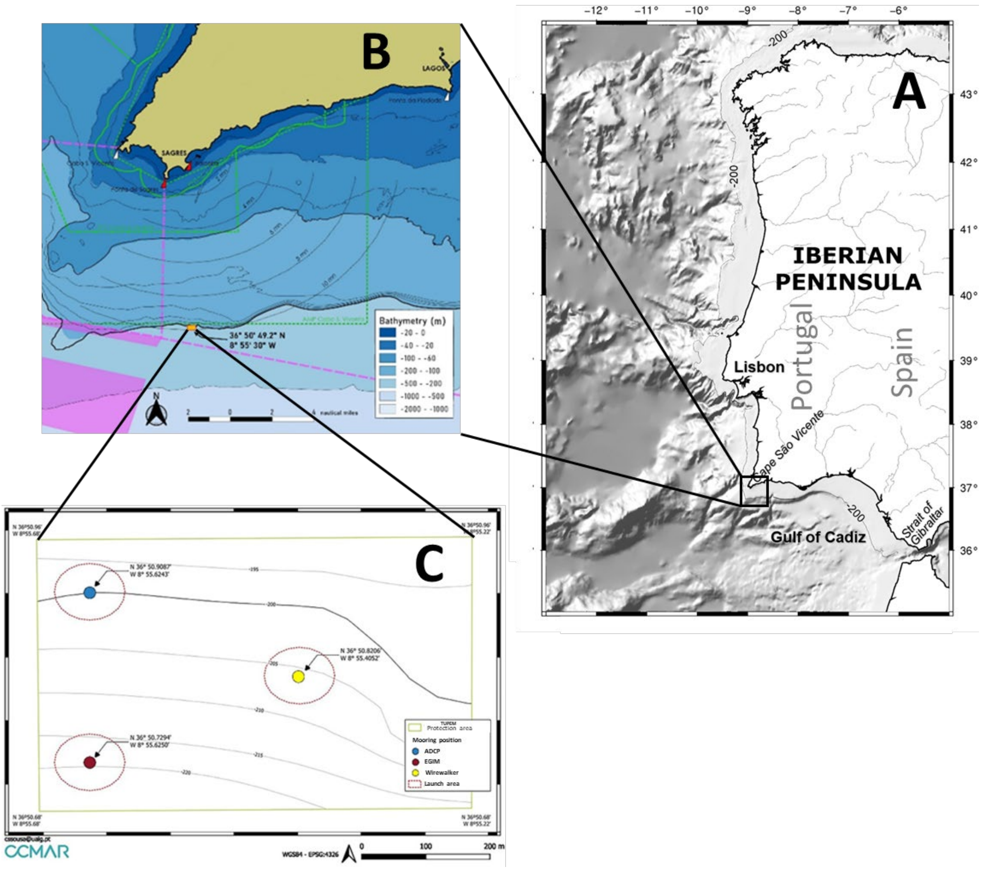

Figure 1. Location of the Cape São Vicente region (**A**). Reserved TUPEM (Permit for Private Use of the National Maritime Space), managed by the Center of Marine Science (CCMAR). Iberian Margin Cape Saint Vicent Ocean Observatory (IbMa-CSV) is located within the TUPEM area (**B**). Mooring sites for each instrument; vertical wave-powered profiler (Wirewalker) (surface, yellow), EGIM (subsurface, red), ADCP (subsurface, blue) (**C**).

An Acoustic Doppler Current Profiler (ADCP) (Teledyne RDI Sentinel V100 300 kHz) mounted in a upward facing subsurface buoy (36.848478 N , -8.927072 E; 150 m), a vertical wave-powered profiler (Wirewalker) (36º50'49.24" N 8º55'24.31" W; near surface to 150 m) and an EMSO Generic Instrument Module (EGIM) (36º50'43.76" N 8º55'37.5" W; 200 m) were deployed from the R/V Mário Ruivo during the EMSO-PT Leg 2 Campaign, in collaboration with the Portuguese Institute for the Sea and Atmosphere, I.P. (IPMA, I.P.), in the TUPEM area during June – October 2022 (Figure 2).

ADCP data were collected every hour for 3 m depth bins (51 bins in total), mounted at 150 m depth (Figure 3). The blank right above the ADCP accounts for 2 m. Ping interval was 1 s and number of pings 120. East-west and north-south component (ms^{-1}) of the current together with the magnitude and direction were acquired. Supplemental parameters, substantial for quality control, are provided

https://doi.org/10.5194/essd-2023-436
Preprint. Discussion started: 18 December 2023

additionally, including correlation, echo intensity and percent of good return of each of the four beams, as well as heading, pitch and roll. The ADCP was further equipped with a thermistor and pressure sensor. The ADCP was calibrated before the deployment according to manufacture guidelines. A 6 channel RBR concerto CTD, equipped with two Turner Designs Cyclops 7F sensors (Chl-a and Turbidty) and one RBRcoda3 T.ODO (optical dissolved oxygen) were installed in a wave powered vertical profiler (Wirewalker) travelling from about 1 m below surface to 150 m depth at an variable speed: upward cast (free floating) ~0.5 ms^{-1}; downward cast (wave motion) ~0.4 ms^{-1} (depending on wave conditions). Sampling rate was 2 Hz ascending, and 10 Hz descending. Measured channels were conductivity, temperature, pressure, chlorophyll a, dissolved O_2 concentration and turbidity. Derived channels are sea pressure, depth, salinity, speed of sound, specific conductivity, dissolved O_2 saturation and density anomaly. An EMSO Generic Instrument Module (EGIM), equipped with a SeaBird SBE37, Aanderaa 4831dw RBR.

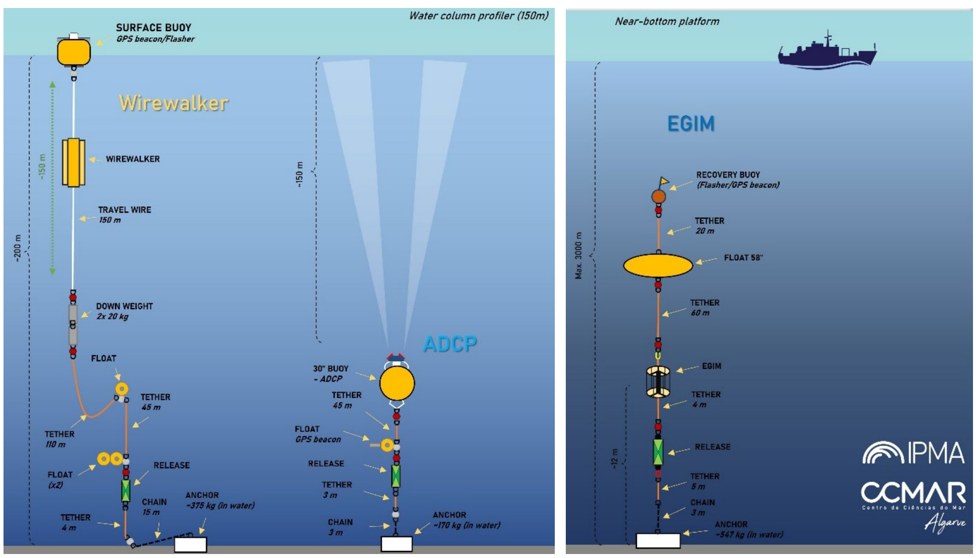

Figure 2. Schematic representation of the IbMa-CSV moorings. Left: Vertical wave profiler and acoustic doppler current profiler, managed by The Center of Marine Science (CCMAR). Right: EMSO Generic Instrument Module, managed by Portuguese Institute for the Sea and Atmosphere (IPMA) and The Center of Marine Science (CCMAR).

Quartz 3 BPR, WETLabs ECO-NTU, OCEANSONICS icListen SB60L-ETH and Teledyne RDI 300kHz Workhorse Monitor direct-reading ADCP was fixed at 200 m. Sampling period was 60 minutes (ADCP), 15 minutes (CT, Turbidity, Oxygen), 30 seconds (Pressure), and 5 minutes / 1 minute recording (acoustics). Measured channels include conductivity, temperature, pressure, temperature, dissolved O_2 concentration, turbidity, currents, and passive acoustics. Derived channels are sea pressure, depth, salinity, speed of sound, specific conductivity, dissolved O_2 saturation and density anomaly. The data time-series from the ADCP and the vertical wave-powered profiler, managed by CCMAR, will be presented in this data paper, along with the description of the data processing and results.

https://doi.org/10.5194/essd-2023-436
Preprint. Discussion started: 18 December 2023

3. Data files and metadata

Instrument data files come in comma-separated value files and are converted into NetCDF format according to CF Conventions 1.6. Files are named after facility code, platform code (WW, EGIM), deployment number (D01, D02, …, Dnn), deployment period, and version (v001, v002, …, vnnn) e.g. [folder_path]\IBMA-CSV_WW_D01_yyyymmdd_to_yyyymmdd_v001.nc. Changes are tracked in a log-text file, which is located in the "dataset type" – directory. Instrument data (raw) are identified with the code "*_v001" and metadata with code "*_M".

The vertical wave-powered profiler data are divided into six NetCDF files, each one approximately two million data points, to keep file size reasonable. Each NetCDF is built upon the same structure: Global attributes, Dimensions and Variables. Global attributes describe the dataset universally through a short descriptive summary as well as other attributes such as temporal extension, geospatial position, principal investigator, person of contact and more (Table 1). Each variable is embedded in one or more dimensions, in this case: Time, Longitude, Latitude, Depth and Bins. Each parameter is accompanied by a set of metadata attributes, holding detailed information about the instrument type, the units and other relevant information regarding the variable. The SeaDataNet parameter discovery vocabulary (https://vocab.seadatanet.org/search), well established in ocean science, is used for attributes, dimensions, variables and units. Further, vocabulary is based on the Copernicus Marine Environment Monitoring Service *In Situ* Thematic Assembly Centre (CMEMS INSTAC) Manual v3.2 and SeaDataNet OceanSITES Data Format Reference Manual v1.4. Common vocabulary facilitates machine-readability and manual findability by users. Each dataset is accompanied by comprehensive metadata. Global and variable specific metadata attributes were agreed upon in the Data Management Service Group (DMSG) of EMSO-ERIC (Table 1). The main objective of EMSO-ERIC DMSG is to assure the findability, accessibility, interoperability and (re)usability of each dataset, according to FAIR standards, harmonize data quality control, format and metadata procedures. Each in this data paper presented dataset can be reused under the CC-BY 4.0 license (https://spdx.org/licenses/CC-BY-4.0).

Table 1. EMSO-ERIC Data Management Service Group Metadata Catalogue.

Global Attributes	Dimensions	Variables	Quality Control
date_created	long_name	long_name	long_name
Conventions	standard_name	standard_name	flag_values
institution_edmo_code	units	units	flag_meanings
institution_edmo_uri	axis	comment	conventions
insitution_ror_uri	ancillary_variables	coordinates	
geospatial_lat_min	sdn_parameter_name	ancillary_variables	
geospatial_lat_max	sdn_parameter_urn	_FillValue	
geospatial_lon_min	sdn_parameter_uri	sdn_parameter_name	
geospatial_lon_max	sdn_uom_name	sdn_parameter_urn	
geospatial_vertical_min	sdn_uom_urn	sdn_parameter_uri	
geospatial_vertical_max	sdn_uom_uri	reference_scale	

https://doi.org/10.5194/essd-2023-436
Preprint. Discussion started: 18 December 2023

time_coverage_start		sdn_uom_name	
time_coverage_end		sdn_uom_urn	
update_interval		sdn_uom_uri	
site_code		sensor_model	
emso_facility		sensor_SeaVoX_L22_code	
source		sensor_reference	
platform_code		sensor_manufacturer	
wmo_platform_code		sensor_manufacturer_urn	
data_type		sensor_manufacturer_uri	
format_version		sensor_serial_number	
network		sensor_mount	
data_mode		sensor_orientation	
title		sensor_depth	
summary		QC_indicator	
keywords			
keywords_vocabulary			
project			
principal_investigator			
principal_investigator_email			
doi			
references			
license			
license_uri			

Quality control variables were created for each measured parameter and for some derived parameters. The quality control variable name is composed of the variable name of the parameter and the suffix "_QC". Quality control procedures and flagging conventions are described in further detail in the next section. For each dataset it was assured that solely measurements, conducted in the water column, are considered. This was achieved by examining depth measurements, derived from the pressure sensor as well as temperatures indicating atmospheric temperatures. Out of water values were removed from each dataset.

4. Technical Validation

Each dataset was subject to quality control (qc). Suspicious and bad values were not removed from the dataset. Instead, a complimentary qc-variable was created, holding flag values describing each individual parameter value. Flag values are defined by the OceanSITES Data Format Reference Manual v1.4 (OceanSITES, 2020). Flag may take the values 0, 1, 2, 3, 4, 7, 8, 9 that are defined as "unknown", "good_data", "probably_good_data", "potentially_correctable bad_data", "bad_data", "nominal_value", "interpolated_value", "missing_value", respectively. In this paper the quality control data is presented. Values that were flagged "potentially_correctable bad_data", "bad_data" and "missing_value" were removed in this paper for presentation purposes.

https://doi.org/10.5194/essd-2023-436
Preprint. Discussion started: 18 December 2023

ADCP quality control was based upon the quality control procedures from Garel *et. al*. (2016). To ensure that no data subject to site lobe interference is shared, the upper 10 % of the data was flagged as "bad_data". Further, the sea surface was detected by locating the cells with a difference among adjacent values greater than three and flagged bad accordingly. This criterion was restricted to cells above the 14th cell (100 m) to prevent misinterpretation of the surface. Cells above and the cell immediately below were flagged as "bad_data". Furthermore, if two or more beams with cells featuring a difference among adjacent bins in echo intensity > 30, and/or with three or more out of four beams with correlation magnitude values lower 64 counts were flagged bad. Temperature was controlled according to SeaDataNet Guidelines (see above) and pressure was assessed via visual inspection.

The first quality control check for the vertical profiler data was done visually via line and boxplots of each variable, allowing a global and regional range check and spike detection at first sight. Quality tests applied on each variable of this dataset were: Sensor range test, global range test, regional range test and spike test. Gradient test was additionally applied to temperature and salinity. Global ranges were obtained from literature for each variable, whereas regional ranges were discussed and selected with regional experts.

Temperature and salinity Spike Test (ST) were conducted according to SeaDataNet Data Quality Control Procedures Manual (SeaDataNet 2010), using the following algorithm: Test value = | V2 - (V3 + V1)/2 | - | (V3 - V1) / 2 | > V THRESHOLD. The value is flagged "bad_data" when the test value exceeds 6 °C, 0.9 PSU, respectively. Gradient Test (GT) relied on the following from SeaDataNet proposed algorithm: Test value = (| V2 - (V1 + V3)/2 | > V_GRAD. The value is flagged "bad_data" when the test value exceeds 9 °C, 1.5 PSU, respectively. Spikes in conductivity were determined by Interquartile Range Test (IQR) (Hald, 1952). Quartile two and quartile three make up the interquartile range (IQR) of the data. Two thresholds are defined for suspicious (1.5) and bad data (3). The IQR is multiplied by each threshold and subtracted (added) from quartile 1 (quartile 3). If a data point exceeds the computed range, it is flagged accordingly. IQR test was not applied on other variables as it was found to be overly sensitive to biogeochemical variables, discarding reasonable values. Therefore, other manuals and standards were used for spike detection in biogeochemical parameters.

Dissolved oxygen, alongside with oxygen saturation, were assessed based on the ST proposed in the Manual for Real-Time Quality Control of Dissolved Oxygen Observations by the Integrated Ocean Observing System (IOOS) Quality Assurance / Quality Control of Real Time Oceanographic Data (QUARTOD) (IOOS QUARTOD, 2018). A spike reference (average of adjacent points DO_{n-2} and DO_n) is subtracted from the tested value (D_{n-1}) and tested against an upper and lower threshold. Values failing the upper boundaries are flagged bad, values in the range of the lower and upper threshold are flagged suspicious. Thresholds for dissolved oxygen and oxygen saturation were set at 4 mgl-1 (lower) and 8 mgl-1(upper) and 80 % (lower) and 120 % (upper), respectively. The most reliable chlorophyll-a spike detection for this dataset is proposed by The Platforms for Biogeochemical studies: Instrumentation and

https://doi.org/10.5194/essd-2023-436
Preprint. Discussion started: 18 December 2023

Measure (PABIM) (PABIM, 2010). The ST algorithm remains the same as in the SeaDataNet Guidelines for temperature and salinity. PABIM (PABIM, 2010) suggests an algorithm to define the threshold value, most appropriate in any region, which is computed as follows: Threshold_Value = |median(V0,V1,V2,V3,V4)| + |σ (V0,V1,V2,V3,V4)|. Turbidity spikes are detected with the same methodology as chlorophyll-a, using a predefined threshold of 6 NTU.

5. Data Records

In this section we visualize the entire data series of the vertical profiles of the of the measured and derived variables in a comprehensive way. Only validated data are displayed. Data considered as bad or potentially bad were not considered to display or for the interpolations, as stated in the previous section. Preliminary analyses as well as basic statistics are presented.

5.1 Acoustic Doppler Current Profiler (ADCP)

Current data from the upward facing ADCP were acquired from June to October 2022 at a depth of 150 m (Figure 3). Measurements above 20 m failed the quality control criteria due to interference with the surface resulting in biased data and were discarded. In the plots we present only the data below 20 m deep (Figure 3). Current meter records demonstrate an energetic current regime in the area south of Cape São Vicente. Clearly, the dominant flow is zonal. The meridional component is weak, without any clear tendency in the direction (notice the different scales of the velocity in Figure 3). The zonal flow shows a prevailing eastward flow, interleaved with sudden inversions to westward. Westward flows are more frequent towards the seafloor.

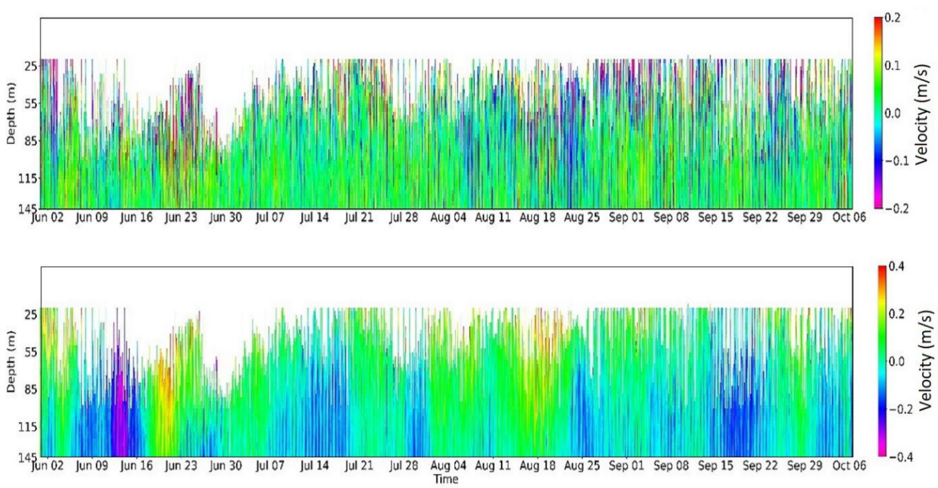

Figure 3. Meridional (north-south) (**top**) and zonal (east-west) (**bottom**) component of acoustic doppler current profiler throughout the whole water column from June to October 2022. White patches reveal absence of valid data. Negative values indicate southward (westward) flow, whereas positive values indicate northward (eastward) flow direction. Measurements are expressed in ms^{-1}. Data above approximately 20 m suffer from surface interference and were removed.

https://doi.org/10.5194/essd-2023-436
Preprint. Discussion started: 18 December 2023

Open Access Earth System Science Data Discussions

Current meter records were divided into three depth ranges to understand the distinctive current regimes along the vertical. The upper layer (UL) comprises the surface waters, reaching down to 60 m. The middle layer (ML) of the water column ranges from 60 to 100 m, and the bottom layer (BL) covers from 100 to 150 m. Polar plots were created for each depth layer to depict the vertical change of the magnitude

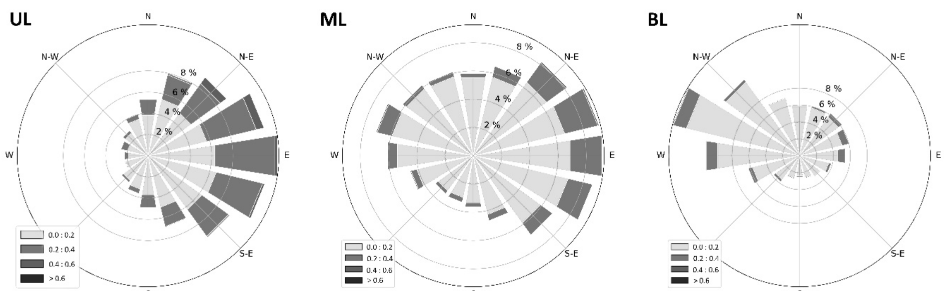

Figure 4. Demonstration of current magnitude and direction of the upper layer (UL; 10 - 60 m), middle layer (ML; 60 – 100m), bottom layer (BL; 100 – 150 m).

and direction of the flow (Figure 4). A relatively energetic flow, showing a few episodes of increased velocities > 0.75 m s^{-1}, prevails in the upper layer. There, the flow shows a strong eastward component, contrasting with the almost absence of westward flow. In the middle layer this prevalence diminishes, and the flow intensity decays, with velocities sporadically reaching values > 0.6 m s^{-1}, but mostly ranging between 0.001 – 0.4 m s^{-1}. As we approach the seafloor, in the bottom layer, the flow is weak, with velocities between 0 and 0.2 m s^{-1}, and a prevailing westward component is evident, opposed to the upper ocean layer. A basic statistic of the flow velocity for each depth interval is presented too. To detail the temporal variability of the mean flow in each depth layer, stick diagrams are presented for each depth layer (Figure 5). The intensified current in the upper layer can be observed throughout the whole period of the deployment. A more diffuse pattern in direction, along with the decrease in velocity can be observed in the lower layers, except for a short period during mid-June. However, there is a prevalence of zonal flow, interrupted periodically by momentary direction changes. June can be identified as the most energetic month in the time series, featuring the highest mean values throughout the water column.

https://doi.org/10.5194/essd-2023-436
Preprint. Discussion started: 18 December 2023

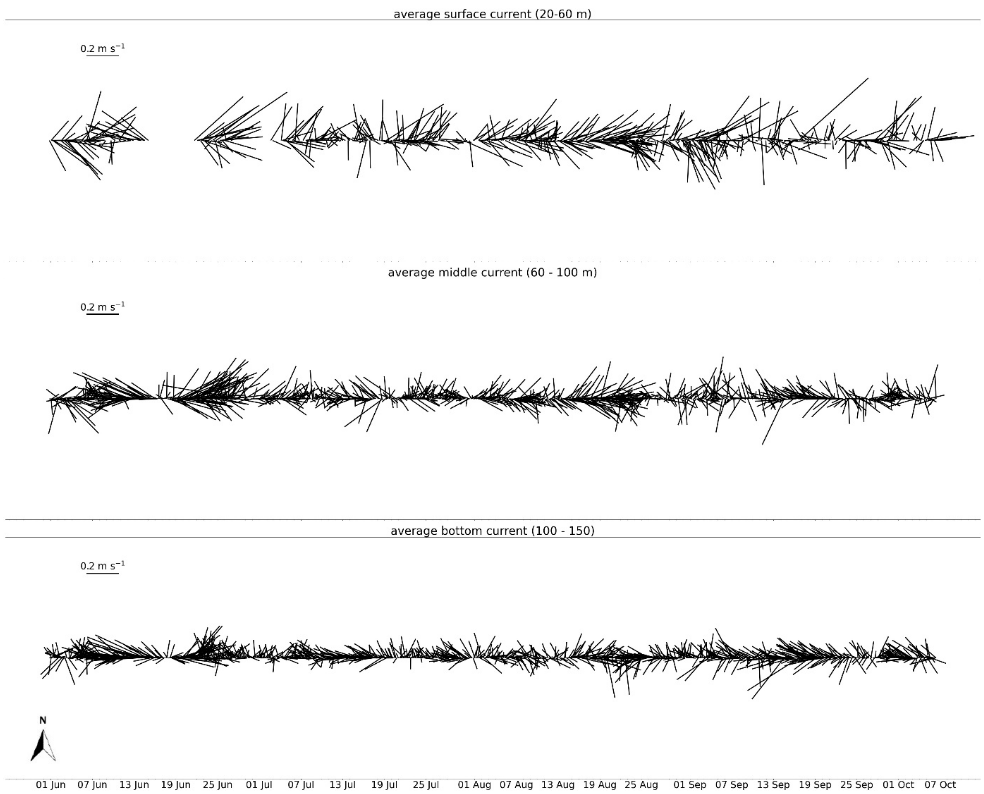

Figure 5. Acoustic doppler current meter stick plot from June to October 2022 divided into upper layer (20-60 m; top), middle layer (60 – 100 m; middle) and bottom layer (100 – 150m; bottom).

Table 2. Statistics of upper layer (UL; 10-60 m), middle layer (ML; 60 – 100m) and bottom layer (BL; 100 – 150 m) grouped by month. SD representing the standard deviation. Values are expressed in ms^{-1}.

	UL				ML				LL			
	Mean	**SD**	**Min**	**Max**	**Mean**	**SD**	**Min**	**Max**	**Mean**	**SD**	**Min**	**Max**
June	0.247	0.105	0.009	0.773	0.186	0.095	0.004	0.574	0.142	0.080	0.001	0.687
July	0.142	0.078	0.002	0.730	0.100	0.059	0.001	0.787	0.089	0.047	0.000	0.509
August	0.182	0.096	0.001	0.639	0.125	0.074	0.000	0.469	0.098	0.053	0.001	0.385
Sept	0.151	0.096	0.003	0.716	0.107	0.059	0.001	0.600	0.101	0.058	0.002	0.510

5.2 Vertical wave-powered profiler (Wirewalker)

Continuous time series of the entire water column are highly valuable as they offer vast amounts of data, and can create a comprehensive picture of mesoscale and sub-mesoscale processes. The vertical wave-powered profiler, equipped with physical and biogeochemical sensors, operated for four months continuously, and delivered a rich dataset at the end of the deployment. Vertical profiles of the water column show temperatures between 12.5 °C closer to the seafloor to approximately 22 °C on the surface (Figure 6; Table 3). The thermocline remains between 20 – 40 m, showing some periods of a well-mixed homogenous surface layer and periods of more stratified waters (Figure 6; Figure 7). Salinities are found

https://doi.org/10.5194/essd-2023-436
Preprint. Discussion started: 18 December 2023

Open Access Earth System Science Data Discussions

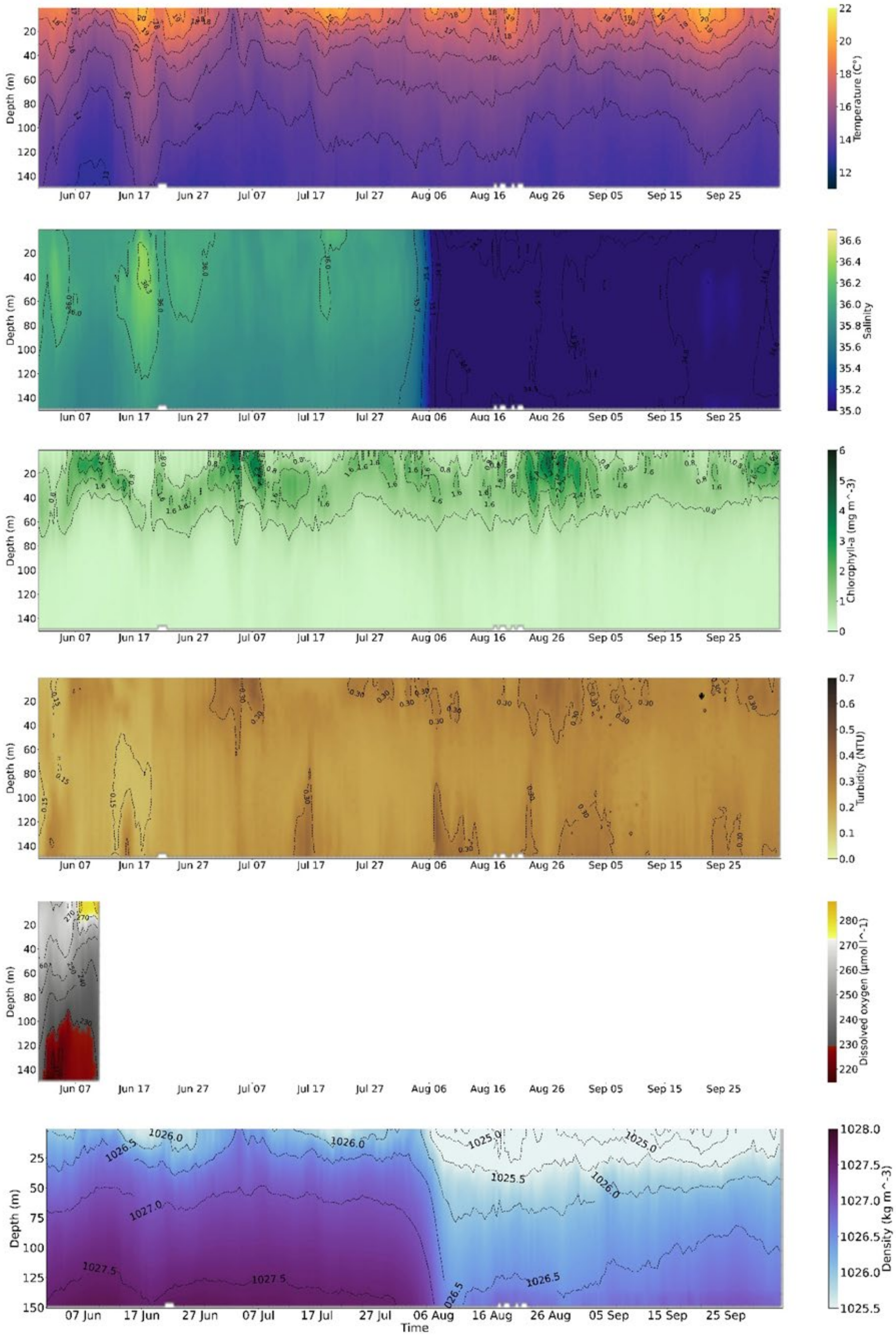

Figure 6. Continuous vertical wave profiler data Jun-Oct 2022. **Top to bottom:** Temperature (°C), salinity, chlorophyll-a concentration (mg m-3), turbidity (NTU), dissolved oxygen (µmol l-1), and density (kg m-3). Salinity and density values after the month of Jul

https://doi.org/10.5194/essd-2023-436
Preprint. Discussion started: 18 December 2023

Open Access Earth System Science Data Discussions

to range between 33 and 37 from June to the end of July with an average salinity of 35.95 (SD ±0.13) and 35.88 (SD ±0.09), respectively (Figure 6; Table 3). Salinity data beyond that point were discarded and will not be discussed further as the conductivity sensor was subject to intense biofouling, prohibiting the collection of trustworthy measurements after the month of July. Due to that the mixed layer depth (MLD) was only computed for the months of June and July, showing an average MLD around the 10-20 m mark, following the pattern of the thermocline (Figure 8, top). The dissolved oxygen sensor shows lower oxygenated waters in deeper waters but stopped operating after two weeks (Figure 6). The chlorophyll-a maximum can be found between 20 - 60 m with concentrations between 1-10 mg m^{-3} and mitigates to almost 0 mg m^{-3} below (Figure 6; Figure *7*; Table 3). Turbidity concentrations correspond

Table 3. Statistics of vertical wave-powered profiler parameters grouped by month. SD representing the standard deviation. Recordings are lacking for the variables dissolved oxygen, oxygen saturation after the first half of June and for salinity after July.

	June				**July**			
	Mean	**SD**	**Min**	**Max**	**Mean**	**SD**	**Min**	**Max**
Temperature (°C)	15.55	1.97	12.62	21.3	15.15	1.7	12.64	20.51
Conductivity (S m^{-1})	4.46	0.21	4.13	5.06	4.41	0.18	4.14	4.98
Salinity	35.95	0.13	34.44	36.72	35.88	0.09	34.13	37.02
Dissolved Oxygen(µmol l^{-1})	245.35	18.5	209.96	305.46	-	-	-	-
Oxygen Saturation (%)	97.77	10.5	81.08	120.0	-	-	-	-
Chlorophyll a (mg m^{-3})	0.59	0.65	0.08	9.33	0.76	0.81	0.09	10.84
Turbidity (NTU)	0.2	0.07	0.0	6.17	0.25	0.09	0.0	6.42
Sound velocity (m s^{-1})	1510.48	5.43	1502.08	1526.23	1509.22	4.62	1502.31	1524.2
	August				**September**			
	Mean	**SD**	**Min**	**Max**	**Mean**	**SD**	**Min**	**Max**
Temperature (°C)	15.41	1.64	12.64	21.56	15.48	2.03	12.74	21.22
Conductivity (S m^{-1})	4.31	0.16	4.01	4.88	4.32	0.19	4.02	4.90
Salinity	-	-	-	-	-	-	-	-
Dissolved Oxygen(µmol l^{-1})	-	-	-	-	-	-	-	-
Oxygen Saturation (%)	-	-	-	-	-	-	-	-
Chlorophyll a (mg m^{-3})	0.83	0.88	0.09	10.51	0.61	0.58	0.08	9.40
Turbidity (NTU)	0.27	0.10	0.04	7.13	0.27	1.41	0.03	363.77
Sound velocity (m s^{-1})	1508.76	4.35	1500.69	1524.31	1508.89	5.44	1501.0	1524.69

to chlorophyll-a during the whole course of the measurements, with average concentrations of 0.25 NTU (SD ±0.17), indicating the correlation between turbidity and biomass with some additional phases of increased turbidity concentrations close to the seafloor (Table 3). In June two period of increased salinity were recorded between the 1^{st} – 6^{th} and 13^{th} to the 21^{st} of June near the surface down to 120 m depth, together with mitigation in chlorophyll-a concentration, migrating to deeper layers along the mixed layer to a depth of approximately 60 m (Figure 6; Figure 8). The salty waters appear in form of an isolated lens, carrying maximum salinities of 36.72 (Figure 6; Figure 7). Simultaneously, an intensification in

https://doi.org/10.5194/essd-2023-436
Preprint. Discussion started: 18 December 2023

stability and spiciness can be observed (Figure 8). Throughout the first half July colder and less saline waters shoal towards the surface with average values of 14.83 ± 1.44 °C and 35.87 ± 0.07, respectively (Figure 6), resulting in a well-mixed and homogenous water column. In response stability and spiciness decrease (Figure 8), accompanied by increasing chlorophyll-a concentration (0.9 ± 1.03 mg m^{-3}) and turbidity (0.26 ± 0.07 NTU). In the second half of the months surface waters experience warming and average increase slightly up to 15.40 ± 1.83 °C, along with an increased stabillity and spiciness (Figure 6; Figure 8). Stratification enhances during August due to a deepening of the warmer surface waters to a depth of approximately 60 m (Figure *8*). Around the 24th of August colder temperate waters shoal towards the surface (19.4 °C), simultaneously with an inflation of the maximum chlorophyll-a concentration (10.51 mg m^{-3}), attenuating in the beginning of September. Upper layer stratification stabilizes throughout the month of September, with temperatures around 21 °C in the upper 40 m with an increased period of warming between the second and third week of the month along with a slight decrease of chlorophyll-a (Figure 6). The same pattern was observed during mid-August, during which, with increased surface temperatures, higher chlorophyll-a concentrations migrate to deeper layers, similar to the third week of July.

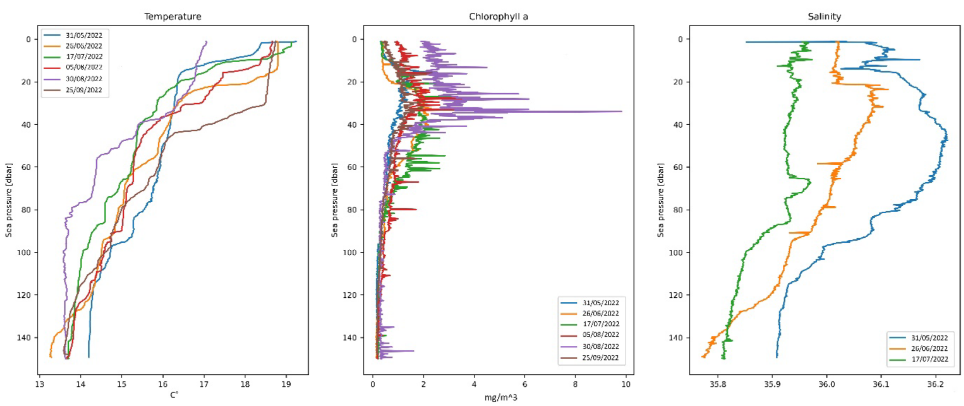

Figure 7. Examples of individual vertical profiles of temperature (C°) (left), chlorophyll-a (mgm-3) (middle) and salinity (right).

6. Data availability

Quality controlled datasets are made publicly available as NetCDF files at the environmental data repository SEANOE (https://www.seanoe.org/) under the DOI https://doi.org/10.17882/94769 in accordance with FAIR principles. Beyond the repository, data is ingested into the CCMAR Erddap server (https://erddap.ccmar.ualg.pt/erddap/index.html), in which a first data visualization and data can be downloaded in various file formats selectively from the user. Further, the data is shared with the EMSO-ERIC Data Portal (https://data.emso.eu/home), in which users can visualize and download data according to their needs. The data is not restricted and is accessible for anyone, accompanied with comprehensive metadata. Standardized datasets allow machine readability and interoperability with various software.

https://doi.org/10.5194/essd-2023-436
Preprint. Discussion started: 18 December 2023

Open Access Earth System Science Data Discussions

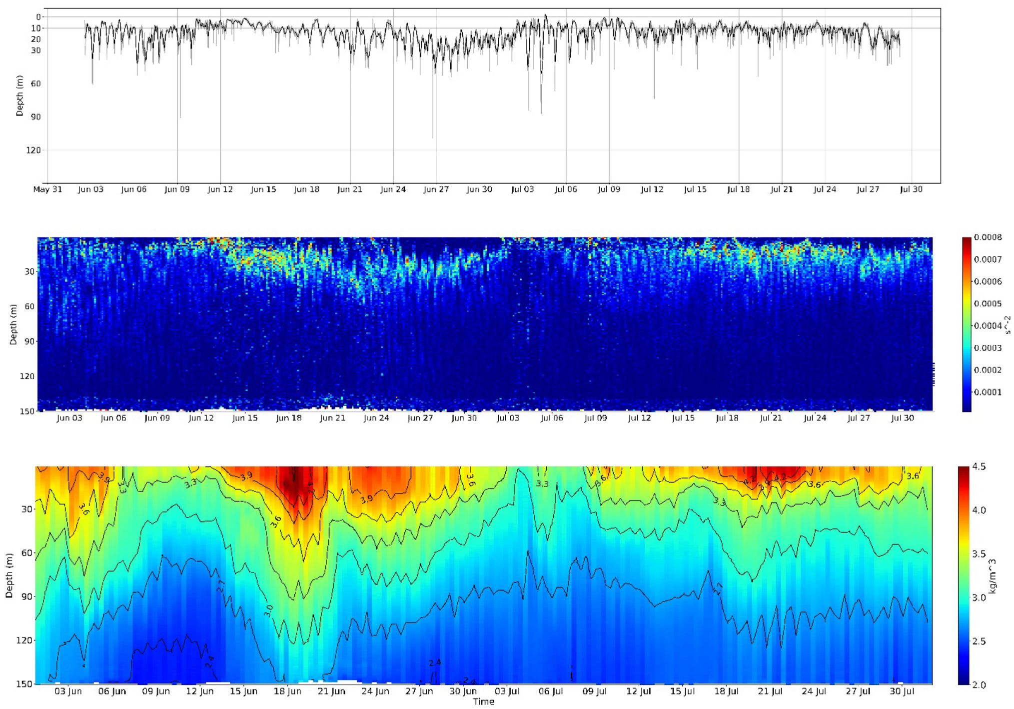

Figure 8. From top to bottom: Mixed layer depth, Brunt-Väisälä frequency (N2), spiciness. Computed for the months of June and July. Subsequent failure of conductivity sensor prohibits computation of presented parameters from that point on.

7. Data set value

This dataset conveys the importance of continuous, long-term data acquisition and ocean monitoring to capture mesoscale and sub-mesoscale events in the ocean. As presented before it was detected, for example during the second half of June, fascinating thermohaline records. This deployment was the first test run of the IbMa-CSV Ocean Observatory. Sensor failure due to biofouling will be tackled by following a regular cleaning of the sensors at specific time intervals while deployed (profiler), and by reducing deployment turn-around with a second vertical wave-powered profiler. Hence, the two profilers will alternate in a minimum four months rhythm, therefore a continuous data collection is guaranteed. The vertical wave-powered profiler offers impeccable high temporal and spatial resolution data products at reasonable cost and maintenance. The only instruments which provide data products with comparable resolution are autonomous underwater vehicles and gliders. Yet economically and regarding the scope of establishing an Eulerian, long-term observation platform, these instruments cannot compete, underpinning the exceptional potential of the vertical wave-powered profiler and its data products.

The monitoring of energetic areas, such as the western tip of the northern margin of the Gulf of Cadiz (the Cape São Vicente), is crucial to understand the complexity of the ocean dynamics and to predict future development via ocean models and their validation through comprehensive datasets. A wide range

https://doi.org/10.5194/essd-2023-436
Preprint. Discussion started: 18 December 2023

of processes, from the upper layers wind induced upwelling to deeper MOW features, do occur in the ocean surrounding Cape São Vicente, as described in the Introduction. Intense mesoscale and sub-mesoscale activity, that represent the "weather" variability of the ocean imposed by the turbulent nature of the circulation, are quite conspicuous in this region and dominates all levels of the water column, challenging the investigation of a wide range of oceanographic processes.

Efforts have been made to develop numerical models for this region, with the aim of better understanding the exchange and mixing processes that occur there, and their implications for the ecosystem and salt spreading in the North Atlantic. However, there is no general theory of turbulence, and numerical models must rely on parametrizations to solve this macro-turbulence. The correct parameterization of the turbulent behavior of the ocean depends on the previous knowledge that we have about the physical characteristics of the region to be modelled. This knowledge is built upon the observation of the ocean. Higher resolution observations will produce better parameterizations of the numerical models. The present data set, with such spatial and temporal resolution, is unique in the region. The present knowledge of the oceanography of the region is inferred from event scale sampling. The parameterization of numerical models in the region is highly data deficient. The parameterization uses analogies with ocean regions with similar oceanographic characteristics and intensively sampled, such as the California Upwelling System. This data series will make it possible to find better parameters for the region and to solve more realistically the turbulence and turbulence related ocean processes.

The IbMa-CSV Ocean Observatory was established in the scope of EMSO-ERIC, a European wide ocean observatory network, and will be further developed and improved to operate continuously and long-term.

9. Usage note

EMSO data are published without any warranty, express or implied. The user assumes all risk arising from his/her use of EMSO data. EMSO data are intended to be research-quality and include estimates of data quality and accuracy, but it is possible that these estimates or the data themselves contain errors. It is the sole responsibility of the user to assess if the data are appropriate for his/her use, and to interpret the data, data quality, and data accuracy accordingly. EMSO welcomes users to ask questions and report problems to the contact addresses listed in the data files or on the EMSO web page.

9. Author Contribution

This research was performed under the framework of EMSO-ERIC. P. Relvas is the principal investigator of the Iberian Margin node of the EMSO-ERIC network. C. Sousa was the technician for the equipment, developed the operational strategy for data collection and, in collaboration with P. Relvas and M. Carapuço, manager of the field activities. M. Carapuço is the coordinator of the research vessels and ocean observatories for the Portuguese Institute for the Sea and Atmosphere and provided of the R/V Mario Ruivo, which was used for data collection. P.Relvas, M. Carapuço and S. Rautenbach assisted during data collection. S. Rautenbach was responsible for the data management, applied FAIR standards to the (meta)data and performed quality control. The manuscript was written by S. Rautenbach, P. Relvas and C. Sousa. M. Carapuço revised and contributed to the manuscript in its final stage.

9. Acknowledgement

This study received Portuguese national funds from: FCT - Foundation for Science and Technology through project UIDB/04326/2020, UIDP/04326/2020 and LA/P/0101/2020; operational programmes CRESC Algarve 2020 and COMPETE 2020 through projects EMBRC.PT ALG-01-0145-FEDER-022121 and EMSO-PT ALG-01-0145-FEDER-022231; EEA Grants Blue Growth project "Atlantic Observatory – Data and Monitoring Infrastructure" (PT-INNOVATION-0002). Furthermore, we would like to acknowledge and thank the R/V Mário Ruivo for the ship-time and support of the crew.

References

Ambar I.: A shallow core of Mediterranean water off western Portugal. Deep-Sea Res 30(6A):677-680, 1983.

Ambar, I., Serra, N., Neves, F., and Ferreira, T.: Observations of the Mediterranean Undercurrent and eddies in the Gulf of Cadiz during 2001, J. Mar. Sys., 71, 195–220, 2008.

Arístegui, J., Álvarez-Salgado, X., Barton, E., Figueiras, F., Hernández-León, S., Roy, C., Santos, A.: Oceanography and fisheries of the Canary Current/Iberian region of the eastern North Atlantic. In: Robinson, A., Brink, K. (Eds.), The Sea, In: The Global Coastal Ocean: Interdisciplinary Regional Studies and Syntheses, vol. 14 (Part B). Harvard University Press, Cambridge, MS, pp. 877–931, 2006.

Bower, A., L. Armi, and Ambar, I.: Direct evidence of meddy formation off the southwestern coast of Portugal. Deep-Sea Res., 42, 1621–1630, 1995.

Cardeira, S., Rita, F., Relvas, P., Cravo, A.: Chlorophyll *a* and chemical signatures during an upwelling event off the South Portuguese coast (SW Iberia). Continental Shelf Research 52, 133–149. 2013. http://doi.org/10.1016/j.csr.2012.11.011

Garel, E.; Laiz, I.; Drago, T.; Relvas, P.: Characterisation of coastal counter-currents on the inner shelf of the Gulf of Cadiz. In: Journal of Marine Systems 155, S. 19–34., 2016

Hald, A., Statistical theory with engineering applications, John Wiley Sons, New York, ISBN-10 0471340561, 1952.

IOOS QUARTOD, Manual for Real-Time Quality Control of Dissolved Oxygen Observations, Version 2.1, August, 2018, https://cdn.ioos.noaa.gov/attachments/2018/08/QARTOD_DOSecondUpdate_final.pdf, (last access: 27 March 2023)

Mauritzen C., Morel Y., Paillet J.: On the influence of Mediterranean water on the central waters of the North Atlantic Ocean , Deep-Sea Research I, vol. 48 (pg. 347-38), 2001.

OceanSITES, Data Format Reference Manual, Version 1.4. ,2020. http://www.oceansites.org/docs/oceansites_data_format_reference_manual.pdf (last access: 27 March 2023)

https://doi.org/10.5194/essd-2023-436
Preprint. Discussion started: 18 December 2023

Open Access Earth System Science Data Discussions

PABIM (Platforms for Biogeochemical studies: Instrumentation and Measure), White book on oceanic autonomous platforms for biogeochemical studies: Instrumentation and measure, Version 1.3, February 2010. https://www.coriolis.eu.org/content/download/3150/23513/file/2009_PABIM_white_book_version1.3.pdf, (last access: 27 March 2023)

Rautenbach S., Relvas P., Sousa C.: EMSO-Iberian Margin Cape St. Vincent observatory data (subsurface mooring) from Jun-Oct 2022. SEANOE. https://doi.org/10.17882/94769 , 2022

Relvas, P., and Barton, E.D.: Mesoscale patterns in the Cape São Vicente (Iberian Peninsula) upwelling region, Journal of Geophysical Research, 107(C10), 3164, doi:10.1029/2000JC000456, 2002.

Relvas, P., and Barton, E.D.: A separated jet and coastal counterflow during upwelling relaxation off Cape São Vicente (Iberian Peninsula), Continental Shelf Research, 25, 29-49, 2005.

Sánchez-Leal, R.F., M. J. Bellanco, L. M. Fernández-Salas, J. García-Lafuente, Gasser-Rubinat M., González-Pola C., Hernández-Molina F. J., Pelegrí, J. L., Peliz A., Relvas P., Roque D., Ruiz-Villarreal M., Sammartino S., Sánchez-Garrido J. C.: The Mediterranean Overflow in the Gulf of Cadiz: A ruggedjourney. Sci. Adv. 3, eaao0609 https://doi.org/10.1126/sciadv.aao0609, 2017

SeaDataNet, Data Quality Control Procedures, 6th Framework of EC DG Research, Version 2.0, May 2010, https://www.seadatanet.org/Standards/Data-Quality-Control (last access: 27 March 2023)

Serra N, Ambar I, Boutov D.: Surface expression of Mediterranean Water dipoles and their contribution to the shelf/slope–open ocean exchange. Ocean Sci 6:191–209, 2010.